NANO LETTERS

Letter

A DNA Nanotransport Device Powered by Polymerase #29

Sudheer Sahu, Thomas H. LaBean, and John H. Reif

Nano Lett., **2008**, 8 (11), 3870-3878 • DOI: 10.1021/nl802294d • Publication Date (Web): 22 October 2008

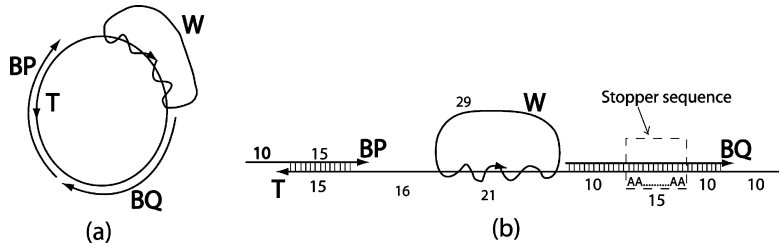

More About This Article

Additional resources and features associated with this article are available within the HTML version:

- Supporting Information
- Access to high resolution figures
- Links to articles and content related to this article
- Copyright permission to reproduce figures and/or text from this article

View the Full Text HTML

Nano Letters is published by the American Chemical Society. 1155 Sixteenth Street N.W., Washington, DC 20036

NANO LETTERS

2008
Vol. 8, No. 11
3870-3878

A DNA Nanotransport Device Powered by Polymerase ϕ29

Sudheer Sahu,[†,§] Thomas H. LaBean,[†,‡] and John H. Reif*[,†]

Department of Computer Science, Box 90129, and Department of Chemistry, 3101 French Family Sciences Center, Box 90345, Duke University, Durham, North Carolina 27708

Received July 29, 2008; Revised Manuscript Received September 24, 2008

ABSTRACT

Polymerases are a family of enzymes responsible for copying or replication of nucleic acids (DNA or RNA) templates and hence sustenance of life processes. In this paper, we present a method to exploit a strand-displacing polymerase ϕ29 as a driving force for nanoscale transportation devices. The principal idea behind the device is strong strand displacement ability of ϕ29, which can displace any DNA strand from its template while extending a primer hybridized to the template. This capability of ϕ29 is used to power the movement of a target nanostructure on a DNA track. The major advantage of using a polymerase driven nanotransportation device as compared to other existing nanorobotical devices is its speed. ϕ29 polymerase can travel at the rate of 2000 nucleotides per minute[1] at room temperature, which translates to approximately 680 nm min^{-1} on a nanostructure. We also demonstrate transportation of a DNA cargo on a DNA track with the help of fluorescence resonance electron transfer data.

1. Introduction. 1.1. DNA Nanorobotics. In recent years, there has been tremendous progress in DNA-based nanodevices.[3,11,12,19,20,25,26,29,30,42,43,53−55] Recent research has explored DNA as a material for self-assembly of nanoscale objects,[10,18,21,24,35,49,51,52] for performing computation,[2,6−8,22,23,47,48,50] and for the construction of nanomechanical devices.[3,11−13,19,25,29,36−39,42,44,45,53,56,57] A potential application of autonomous DNA nanorobotical devices is in the design of a controllable moving device integrated into a DNA lattice for efficient transportation of nanoscale materials.

1.2. Polymerase as a Machine. We have known polymerase as an enzyme responsible for the copying and replication of DNA or RNA template. Polymerase copies sequence information of DNA or RNA by extending a primer hybridized to the template by adding available free complementary nucleotides to its 3′ end.

Researchers have been interested in understanding the exact mechanism of polymerase for extension of primer, and the mechanical properties related to primer extension. Gelles et al.[14] reviewed RNA polymerase movements during transcription and studied mechanisms of RNA polymerase translocation along DNA. Wang et al.[46] measured force and velocity for single molecules of RNA polymerase. Many researchers preferred to view the polymerase as a machine and studied the mechanisms of their movements. Most notably, Spirin[40] considered the structure and functions of RNA in terms of a conveying molecular machine. He studied the principal scheme of forward movement of RNA polymerase along the DNA template. Binding of substrates and utilization of energy from chemical reactions provide successive selection and fixation for subsequent conformational states of enzyme complex. This in turn provides directionality by means of a "Brownian ratchet mechanism". Goel[15] revealed through a series of single-molecule experiments that mechanical tension on DNA can control both the speed and direction of the DNA polymerase motor. Thomen et al.[41] addressed the issue of how the enzyme converts chemical energy into motion.

In these experiments, mechanical properties of various polymerase enzymes were explored. However, in none of these studies was the mechanical energy of the polymerase harnessed or exploited to transport other objects.

1.3. Our Contribution. In this paper, we present the first design of a nanotransportation device powered by a polymerase. We use ϕ29, a polymerase known for its exceptional strand displacement activity, to push a DNA cargo. Researchers have studied the structure of ϕ29 polymerase, have provided useful insights into its exceptional strand displacement and processivity, and have deduced its translocation mechanism.[9,16,17,32]

In section 2.1 we describe the basic principle of our nanotransportation device, and in section 2.2 we describe a high-level design of the device. In section 3, we outline

* Corresponding author, reif@cs.duke.edu.
† Department of Computer Science.
‡ Department of Chemistry.
§ The author contributed to the research mentioned in this article when he was a Ph.D student at Duke University.

10.1021/nl802294d CCC: $40.75
Published on Web 10/22/2008

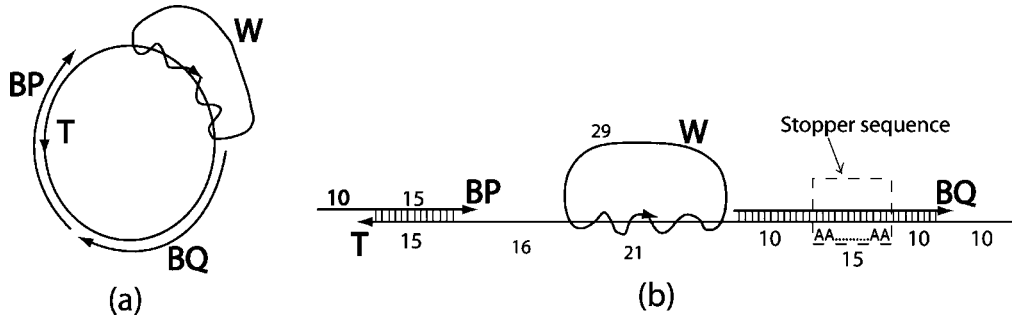

Figure 1. (a) Basic design of the polymerase-driven nanotransportation device. Polymerase extends the primer BP, and pushes the wheel W on the track T. Protector strand BQ prevents the wheel from moving on its own but is dislodged by polymerase extension of BP on left. (b) The design of a polymerase-based nanotransportation device in terms of lengths of DNA sequences

experimental materials and methods. In section 4, we discuss our experimental results in detail.

2. Our Polymerase ϕ29 Based Nanotransportation Device. 2.1. Basic Principle. With our polymerase-driven nanotransportation device, we aim to exploit the mechanical energy of polymerase when it travels toward the 5′ end of DNA tracks. Another DNA strand (DNA cargo), when attached to the template blocking the path of polymerase, is pushed by the moving polymerase. Polymerase ϕ29 is our choice for pushing the cargo. Figure 1a illustrates the basic idea of our ϕ29 polymerase nanotransportation device.

In order to brake this polymerase nanotransportation device at a desired destination, we use a sequence of consecutive A's (known as *stopping sequence*) on the template. The template does not contain any A's before the stopping sequence. If the reaction solution lacks the nucleotide T, then the polymerase can still extend the primer until the beginning of the stopping sequence but cannot advance further, and hence the device stops.

The major advantage of using a polymerase-driven motor over other nanorobotical devices is its speed. ϕ29 polymerase can travel at the rate of 2000 nucleotides per minute at room temperature,[1] which is equivalent to approximately 680 nm min^{-1}.

2.2. Design of a ϕ29 Polymerase Nanotransportation Device. Figure 1a illustrates the basic design of our polymerase based nanotransportation device. The polymerase pushes the wheel cargo on the track (template). It should be noted that the wheel does not roll on the track. It is intertwined with the track and gets pushed without rolling. The wheel has a 21 bases (two helical turns) long complementary sequence to the region of track only near its initial position. Therefore it hybridizes with the template track only at the initial position and nowhere after that. The hybridization site is needed to ensure that the wheel is initially attached to the track at a unique position. However, once the wheel has been displaced from its initial position, it can just slip on the track arbitrarily even without a push from polymerase. In order to prevent the wheel from slipping away on the track on its own, a strand BQ, referred to as the *protector strand*, is hybridized on the downstream region of the track. It is shown in Figure 1a. Another purpose of strand BQ is to impart rigidity to the track, which otherwise might fold onto itself.

Figure 1b shows more details of the system. The track is chosen to be a DNA strand of length approximately 100 bases. The wheel hybridizes with track in a 21 base long region, which is 45 bases away from the 5′ end of the track, as shown in Figure 1b. The strand BP is a 25 bases long primer that hybridizes to the track, T, as shown in Figure 1b. A free space of 16 bases is left so there is room for the polymerase to bind. There is a sequence of 15 consecutive A's in the track, T, that act as the stopping sequence. The total length of the wheel strand is 50 bases, and the protector strand BQ is 35 bases long.

We would like to point out a few design constraints before we describe the experimental methods in section 3. There should not be any A's in the track between the initial position of the polymerase and the stopping sequence, so that the polymerase does not stop before the desired position. We used the primer of length more than six bases for polymerase ϕ29 as recommended by the manufacturer. For circularization of a single strand DNA (for constructing the wheel), a length greater than 40 bases is preferred. For the polymerase ϕ29 the recommended temperature is 30 °C. At 25 °C, there is a 5% loss in efficiency. Protector strand BQ should have dideoxynucleotide (ddNTP) at its 3′ end in order to prevent extension by polymerase ϕ29.

3. Overview of Experiments. The very first challenge is to assemble the circular wheel strand on a linear track strand. The 5′ end of the wheel needs to be phosphorylated so that it can be ligated with its 3′ end and form a complete circle. If the wheel is already circularized, the track must be threaded through the wheel to form a double helical region; this can be extremely challenging experimentally. Therefore, we use a technique known as padlock probes[27,4] to attach circular wheel to the track. The track acts as a linker for circularization of linear wheel strand by hybridizing with both ends of the wheel, which can then be ligated with each other to form a circle.

In order to ensure that the wheel is always attached to the track, we circularize the track as well by ligating its two ends together. The circular wheel is in an intertwined conformation with the circularized track and hence does not detach from it. The fact that the track and the wheel are inseparable from each other makes it easier for us to detect the assembly in a denaturing gel. It also ensures that the wheel stays on the track during the experiment.

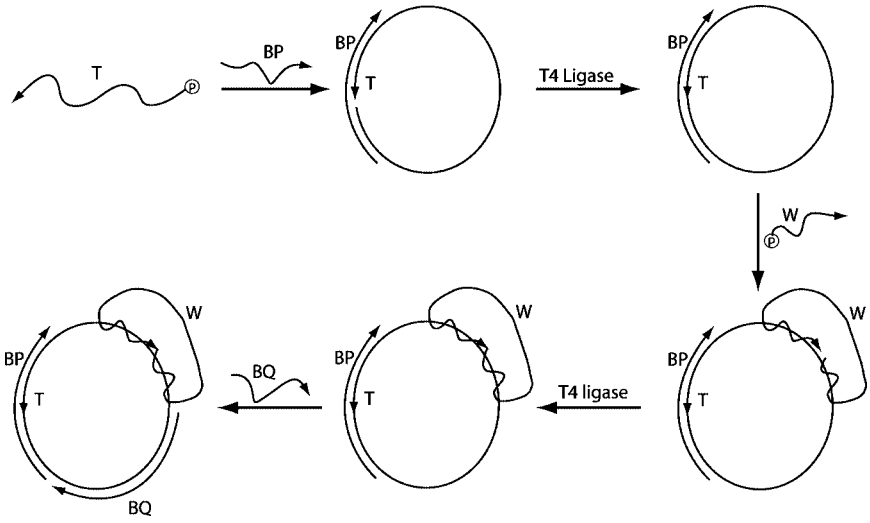

Figure 2. Overview of the complete setup assembly of polymerase based nanotransportation device.

We are able to use a strand BP simultaneously as a linker and a primer. Figure 2 summarizes the entire process. Track strand T is first circularized using the linker-cum-primer strand BP, and then ligated using T4 ligase. In the next step, the wheel strand is circularized using the track strand T as the linker, as shown in Figure 2. This is done by hybridization of the linear strand W with circularized T, followed by its ligation to seal the nick in it. It should be noted that the presence of the phosphate groups at the 5′ ends is required for these circularizations.

The next step is the hybridization of protector strand BQ onto this assembly. It should be noted that ddNTP (dideoxy-NTP) is required at the end of strand BQ to prevent it from extending under the influence of polymerase. As mentioned earlier, we leave a space of 16 bases between the strand BP and the wheel on the track in which polymerase ϕ29 can bind. The wheel is chosen to be 50 bases so that it can be easily circularized. The track contains 15 consecutive A's as the stopping sequence. It is expected that in the presence of all four nucleotides in the reaction solution, the polymerase ϕ29 will continue extending the primer and circling on the circular track, while displacing any strand that comes in its way. This results in a rolling circle amplification, as described in section 4.

Experimental protocols and the sequences of all strands used here are given in Supporting Information.

4. Results and Discussion. Construction of a Circular Track Using a Linker Strand. Three μM T and 3 μM BP were annealed together in 1X TAE buffer. The solution was heated to 90 °C and then cooled down to the room temperature over a period of 4 h. It was then ligated with T4 ligase to obtain circularized T. Small aliquots were taken from the resultant solution to analyze in 10% denaturing gel (run at 50 °C at 220 V for 1.5 h). Figure 3a shows strands BP and T against T.BP (ligated) in the denaturing gel. In the T.BP column, the topmost band corresponds to circular track. The strand BP separates from the circular track in denaturing gel and can be seen at the same height as BP in Figure 3a.

Attachment of Wheel onto the Circular Track. Strand W is added to the circular track and is circularized using padlock probe method. W is annealed with T.BP at 1.2 μM for 4 h (cooling from 80 °C to room temperature) in presence of 1X TAE buffer. It was then ligated with T4 ligase. Thus we have the product T.BP.W(*ligated*) formed with two ends of W ligated with each other.

The product was analyzed using 10% denaturing gel as shown in Figure 3b. The wheel and the track are intertwined with each other as desired. In Figure 3b, the topmost bands in wells labeled as T.BP.W are circularized wheel and circularized track intertwined with each other.

Action of Polymerase ϕ29. T.BP.W solution from previous step was annealed with an equimolar solution of BQ in presence of 1X TAE.Mg buffer. The solution was annealed (heated to 75 °C and cooled down to room temperature over 2 h). Multiple samples were drawn from it for various experiments of polymerase ϕ29 under different conditions.

First of all, four samples of T.BP.W.BQ were prepared, and ϕ29 polymerase with polymerase buffer, BSA, and dNTPs were added to them as follows: the first sample contained all the dNTPs, the second sample contained all but T, the third lacked C and T, and the fourth sample had only nucleotide A in it.

The 10% native gel in Figure 4a shows the T.BP.W.BQ sample with four nucleotides exhibits the phenomenon of rolling circle amplification, due to the extension of the strand BP on the circular track. The presence of multiple bands in the case of T.BP.W.BQ implies the formation of various intermediate products, but the rolling circle product formed on T.BP.W.BQ in the presence of four nucleotides and polymerase ϕ29 is most dominant.

The wheel and the track are already ligated to form a circle, the only primers in our setup are the strands BP and BQ. The rolling circle amplification indicates the extension of only these two strands. We have already shown in section 4 that wheel and track formed two circles intertwined with each other (inseparable in a denaturing gel). Therefore, the circular motion of the polymerase on the circular track during

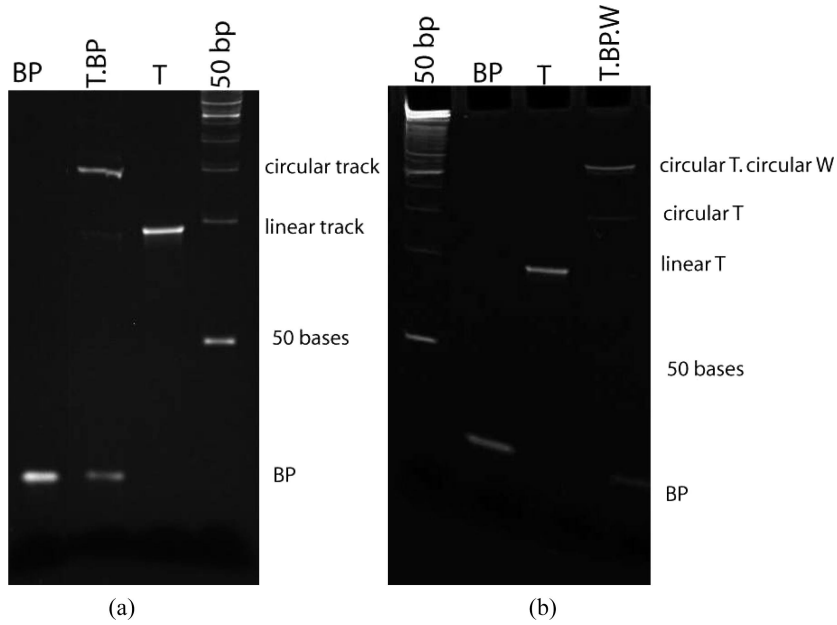

Figure 3. Strand T circularized using linker strand BP. The bottom-most bands correspond to BP. And it is marked against a 50 bp ladder. (b) Strand W is hybridized with T.BP, as shown in Figure 2, and subsequently ligated to form a circular wheel and a circular track intertwined with each other. Denaturing gel is unable to separate them.

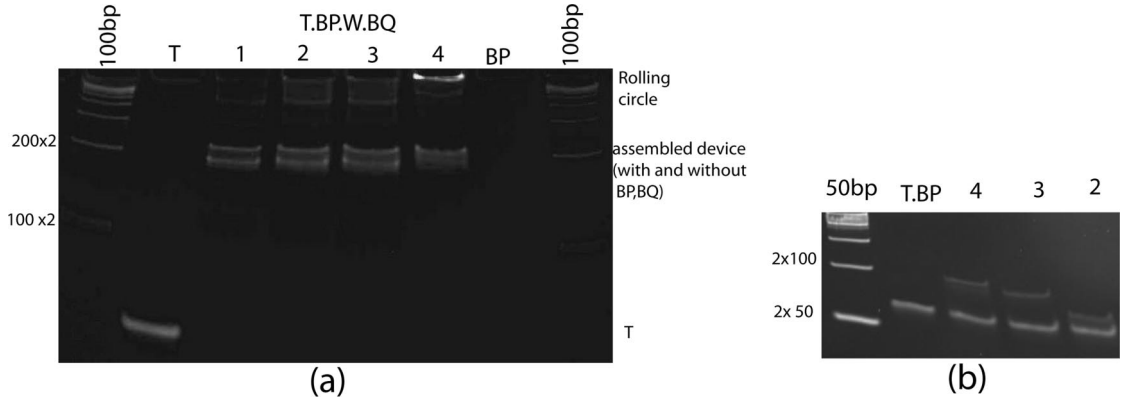

Figure 4. (a) Polymerase ϕ29 acts on T.BP.W.BQ in the presence of one, two, three, and four dNTPs. (b) The effect of reducing the quantity of ϕ29 on braking. Polymerase ϕ29 acts on T.BP in the presence of two, three, and four dNTPs.

the rolling circle amplification should imply that the wheel gets pushed on the track by polymerase, due to the strong strand displacement properties of the ϕ29 polymerase.

Brakes on Polymerase-Driven Nanotransportation Device. The stopping mechanism is based on a sequence of 15 consecutive A's on the track and the lack of the dNTP T in the reaction mixture. It causes the polymerase to get stuck at the stopping sequence and in effect stops or brakes the nanotransportation device. We performed a series of experiments to test the efficiency of this braking mechanism and to determine the conditions favorable for it.

T and BP were annealed from 90 °C to room temperature over a period of 2 h to form T.BP. Four samples of T.BP were drawn from it, and ϕ29 polymerase with polymerase buffer, BSA, and dNTPs were added to them as follows: the first sample contained all the dNTPs, the second sample contained all but T, the third lacked C and T, and the fourth sample had only nucleotide A in it. The samples were incubated at 30 °C for 30 min, and then polymerase was deactivated by heating to 65 °C for 10 min.

It was observed that ϕ29 did not work well with our braking mechanism, when taken in excess of 30 units/mL. The exonuclease part of the polymerase that is responsible for proofreading does not work so well if ϕ29 is in excess. No difference was visible in the product formed in the presence of all four dNTPs vs three dNTPs. It completes one full circle whether all four nucleotides are present or only three nucleotides are present. In such conditions, whenever ϕ29 does not find the correct base, it adds incorrect bases to extend the primer and proceeds further. The inability of ϕ29 to stop at a stopping sequence of consecutive A's in the absence of T in the presence of excess ϕ29 is poorly understood, and exploring it is beyond the scope of this work.

However, a lower concentration of ϕ29 is favorable for our braking mechanism. A similar experiment with a quantity of

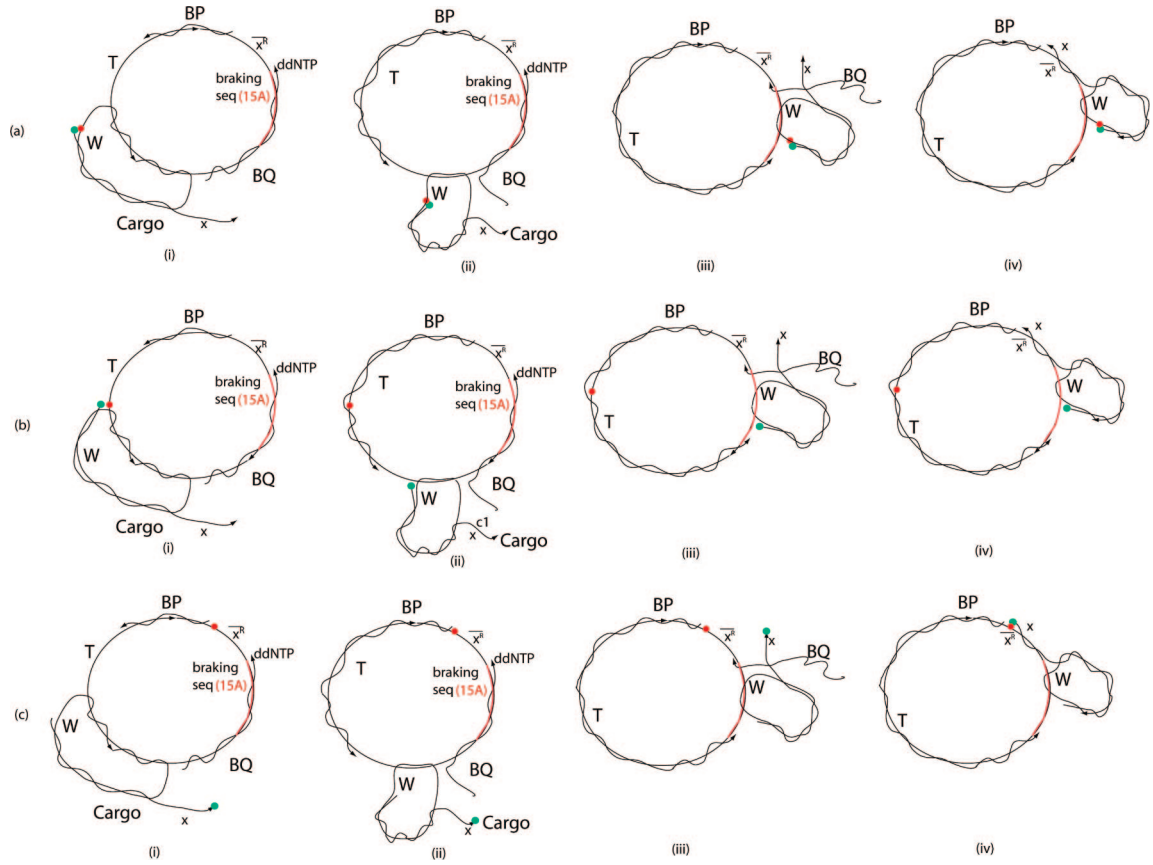

Figure 5. (a) Fluorescence experiment that shows that the cargo is not dislodged from the wheel W. (b) Fluorescence experiment that shows that the wheel and the cargo move from their initial positions. (c) Fluorescence experiment that shows that the wheel and the cargo reach the final desired position.

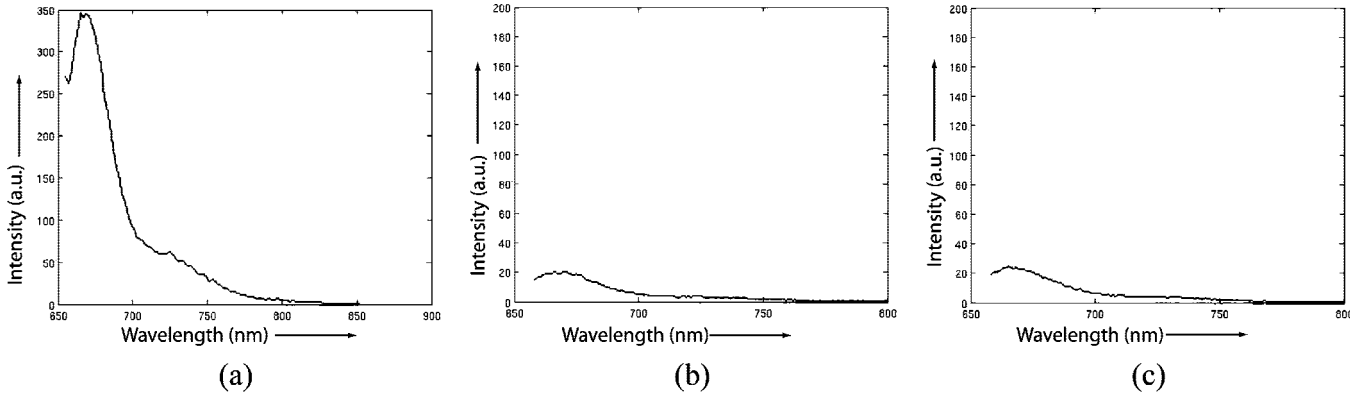

Figure 6. (a) The fluorescence shown by the assembly in the absence of the cargo containing the quencher. (b) The fluorescence quenched by the assembly of cargo containing the quencher. (c) The fluorescence remains quenched even after the activity of the polymerase ϕ29, which indicates that the cargo is not dislodged from the wheel W.

ϕ29 decreased to 23 units/mL in its samples was performed. The samples as analyzed in 10% native gel are shown in Figure 4b. It can be seen that in ϕ29 samples, in the presence of two, three, or four dNTPs, different products are formed, shown by the existence of different bands in Figure 4b. With four nucleotides, it completes one full circle, while with three nucleotides, it stops at the stopping sequence, and with two nucleotides it stops even earlier. Thus at this concentration of ϕ29, the braking mechanism works well.

As an aside, we observed that ϕ29 polymerase is not able to extend the primer beyond a nick, and therefore no rolling circle amplification is observed. Figure 4b shows that in the case of T.BP, the longest product formed on extension by polymerase ϕ29 is approximately 200 bases in weight.

FRET Experiments on our Polymerase-Based Nanotransportation Device. The PAGE analysis presented in previous sections presents an indirect method to verify the

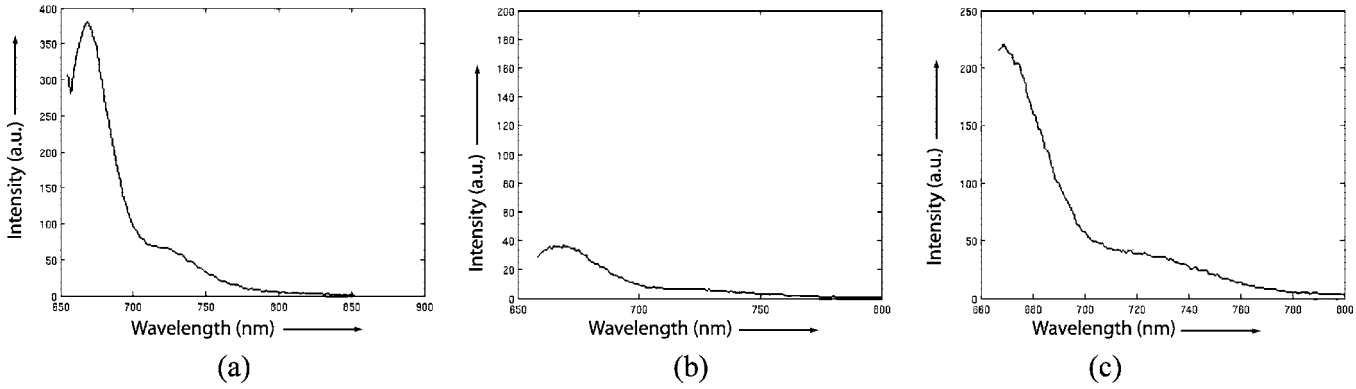

Figure 7. (a) The fluorescence is shown by the assembly in absence of the cargo containing the quencher. (b) The fluorescence is quenched after the assembly of the cargo containing the quencher. (c) The fluorescence reappears after the polymerase $\phi 29$ pushes the wheel containing the quencher.

Table 1. DNA Sequences for the Demonstration of Polymerase-Based Nanotransportation Device

symbol	sequence
T	/5Phos/AAT CAC CAT AGT GCA ACC TGA AAA AAA AAA AAA AAT GTG CCT CTG TTC TGC TCG CTT GCT GCG TTG GCT GTC GTG TCC TTG TTA CTA AGA TGC TTA C
W	/5Phos/AGC GAG CAG AAA AAA AAA AAA AAA AAA AAA AAA AAA CCA ACG CAG CA
BQ	CAG AGG CAC ATT TTT TTT TTT TTT TCA GGT TGC AC
BP	TAT GGT GAT TGT AAG CAT CTT AGT A
PM3.T	/5Phos/AAT CAC CAT AGT GCA ACC TGA AAA AAA AAA AAA AAT GTG CCT CTG TTC TGC TCG CTT GCT GCG TTG GCT GTC GTG TCC TTG TTA CTA AGA TGC TTA C
PM3.W	/5Phos/ AGC GAG CAG AAT GCA GTC ACA CTG AGA TCG AGA CT/iCy5/T GTA CCA ACG CAG CA
PM3.Cargo	/5IAbRQ/AGT CTC GAT CTC AGT GTG ACC AGG TTG CAC
PM3.BQ	CAG AGG CAC ATT TTT TTT TTT TTT T
PM3.BP	TAT GGT GAT TGT AAG CAT CTT AGT A
PM2.Track	/5Phos/ T GTG CCT CTG TTC TGC TCG CTT GCT GCG TTG G /iCy5/CT GTC GTG TCC TTG TTA CTA AGA TGC TTA CAAT CAC CAT AGT GCA ACC TGA AAA AAA AAA AAA AA
PM2.Wheel	/5Phos/ AGC GAG CAG AAT GCA GTC ACA CTG AGA TCG AGA CTT GTA CCA ACG CAG CA
PM2.Cargo	/5IAbRQ/ TACA AGT CTC GAT CTC AGT GTG ACC AGG TTG CAC
PM2.BQ	CAG AGG CAC ATT TTT TTT TTT TTT T
PM2.BP	TAT GGT GAT TGT AAG CAT CTT AGT A
PM1.T	/5Phos/AAT CAC CAT A/iCy5/GT GCA ACC TGA AAA AAA AAA AAA AAT GTG CCT CTG TTC TGC TCG CTT GCT GCG TTG GCT GTC GTG TCC TTG TTA CTA AGA TGC TTA C
PM1.W	/5Phos/ AGC GAG CAG AAT GCA GTC ACA CTG AGA TCG AGA CTT GTA CCA ACG CAG CA
PM1.Cargo	AGT CTC GAT CTC AGT GTG ACC AGG TTG CAC/3IAbRQSp/
PM1.BQ	CAG AGG CAC ATT TTT TTT TTT TTT T
PM1.BP	TAT GGT GAT TGT AAG CAT CTT AGT A

activity of a polymerase-based nanotransportation device. In this section, we present FRET (fluorescence resonance energy transfer)-based methods for verification of our nanotransportation device. For FRET experiments on our polymerase-based nanotransportation device, the wheel carries a cargo with a quencher on one of its ends, and the fluorophore is located on the track or wheel. The sequence level detail of the construction for FRET experiments is given in Supporting Information in Figure 10.

1. Demonstration That the Cargo Was Not Dislodged from the Wheel. This is demonstrated by having a quencher in the cargo at the 5′ end and a fluorophore in the wheel at the corresponding position as shown in Figure 5a. Initially, the complete device except the cargo (containing the quencher) is assembled, and the fluorescence is measured. Figure 6a shows the fluorescence in the assembly in the absence of the cargo. The cargo is then assembled onto the wheel resulting in the structure shown in Figure 5a. The fluorescence measurement of the assembled structure is shown in Figure 6b. All fluorescence is quenched. After the extension of the primer by polymerase $\phi 29$, the fluorescence is measured again (Figure 6c)). The fact that it still shows no fluorescence indicates that the cargo is not dislodged from the wheel.

2. Demonstration That the Wheel Was Pushed from the Initial Position. Figure 5b shows the entire procedure. The 5′ end of cargo contains the quencher, and the track has *iCy5*\ fluorophore at the 32nd nucleotide. The position of the internal fluorophore is the 32nd base. The cargo strand in this experiment is 34 bases long instead of 30, with an

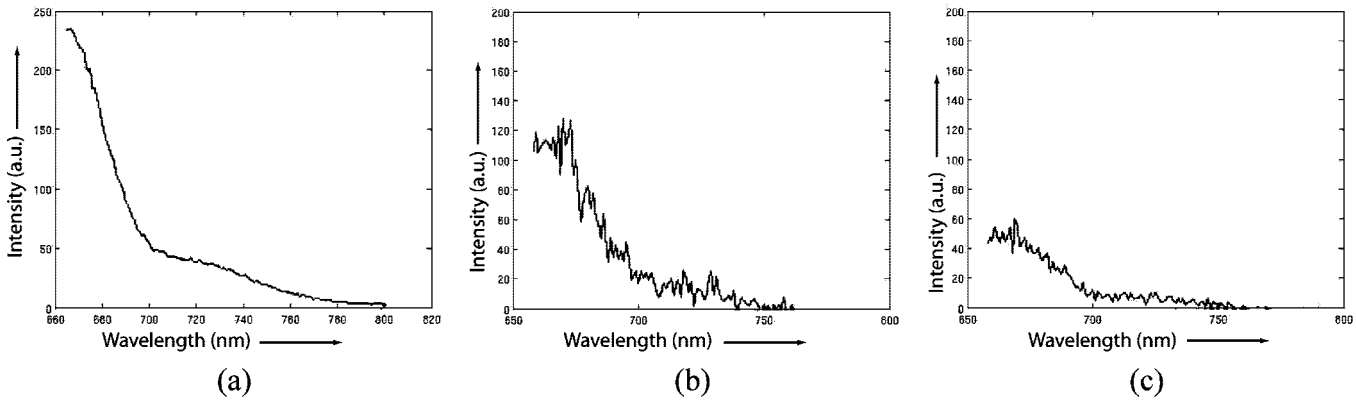

Figure 8. (a) The fluorescence is shown by the assembly in the absence of the cargo containing the quencher. (b) The fluorescence remains after the assembly of the cargo containing the quencher, away from the fluorophore. (c) The fluorescence quenches after the polymerase ϕ29 pushes the wheel before it stops at the stopping sequence, and the sticky end of the cargo hybridizes with the track to quench the fluorescence.

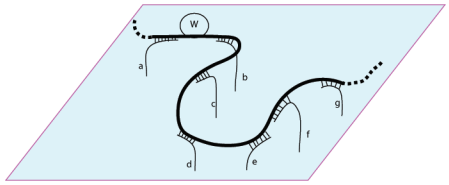

Figure 9. (a) A schematic showing a programmable arbitrary track laid on top of an addressable two-dimensional nanostructure from DNA origami (gray surface). The dangler strands are shown using thin lines, and they have free ends that protrude out of the nanostructure. The track is shown using a bold line that partially hybridizes with the dangler strands in a desirable manner.

additional complementary fragment added at the 5′ side tailored for this experiment. Iowa Black RQ quencher is attached to the 5′ end.

Initially, the complete assembly except the cargo is constructed, and the fluorescence measurement is taken (Figure 7a). On the assembly of the cargo onto the wheel, the fluorescence is quenched as shown in Figure 7b. But after the extension of primer by polymerase ϕ29, the fluorescence can be observed again as shown in Figure 7c. This indicates that now the cargo is not close to the fluorophore. We have already shown in the previous section that cargo is not dislodged from the wheel; therefore, it means that wheel is no longer close to the fluorophore. This implies that the wheel is indeed pushed from its initial position.

3. Demonstration That the Wheel Reached the Desired Final Position. Figure 5c illustrates the entire procedure. The sequences are shown in Table 1. The quencher Iowa Black RQ is incorporated at the 3′ end of the cargo, which is a 30mer, and the track has /*iCy*5/ fluorophore at the 11th nucleotide. The difference in the design is because of difficulties in synthesis of oligonucleotides with /*iCy*5/ away from the 5′ end.

Initially, the complete device (Figure 5c) without the cargo is assembled. As expected, the fluorescence is observed as shown in Figure 8a. Then, low-temperature annealing (heated to 45 °C and then cooled) is performed to assemble the cargo on the track, without the removal of PM1.BQ from the track. Even now, the fluorescence is present, albeit reduced (Figure 8b). However, once the polymerase ϕ29 is added to the solution and the primer BP is extended, the fluorescence is quenched (Figure 8c). This indicated that the wheel reached the desired final destination.

However, it should be noted that the assembly of cargo (containing the quencher) resulted in reduction of some fluorescence (Figure 8, panels a to b). This is because of the hybridization of the sticky end, x, of the cargo with the $\bar{x}$ subsequence of the track T. One of the purposes of PM1.BQ was to provide rigidity to the track in order to prevent this from happening, but it does not seem to be foolproof. The problem in using our earlier version of BQ is that it will protect the $\bar{x}$ part of sequence permanently, and hence, it might not be available to the cargo at the end.

5. Discussion and Future Work. We demonstrated the functioning of a promising nanoscale motor device. The main advantage of using a polymerase-driven motor is its speed. As compared to other existing molecular motors based on ligation restriction,[55,5] DNAzymes,[43,12,42] and fuel-strands,[36−39,44,45,56,57] a polymerase-driven nanotransportation device is much faster. The more popular Taq polymerase is unfit for such an application because of the lack of significant strand displacement activity in it. However we found that ϕ29 polymerase does not show good exonuclease activity when present in excess, which causes low fidelity. We also found that ϕ29 does not extend a primer across a nick in the template.

An immediate future goal is to demonstrate two-dimensional routing of the polymerase nanotransportation device. It may be achieved by demonstrating the motion of the polymerase powered nanotransportation device on DNA origami[33] and addressable lattices. Two dimensional nanostructures from DNA origami provides the basic platform. They can be conveniently replaced by two-dimensional addressable lattices formed using 4 × 4 tiles[28] for our purpose. Our idea is to implant a series of single-stranded DNA stator strands on the two-dimensional plane so that a track can be assembled on top of the stator strands, as illustrated in Figure 1.

Thus, a polymerase-based nanotransportation device can provide transport between arbitrary points on a two-dimensional nanostructure along an arbitrary path.

Furthermore, the wheel can be used for nanoparticle transportation by using appropriate attachment chemistry. Loading and unloading mechanisms for cargos on the wheel can be designed using strand displacement as described in ref 31.

Another extension to a polymerase-based nanotransportation device is to make it programmable in the sense that it has the capability of making decisions on choosing a path from among multiple paths. Equally important is to impart back and forth shuttling capabilities to the polymerase motor. Then a possible application of the polymerase-powered nanotransportation device can be in the construction of nanoshuttles. Arbitrary tracks analogous to the railway tracks can be laid out on nanostructures, and we might have multiple polymerase nanoshuttles working in tandem carrying out nanoscale transportation in a programmable and efficient manner.

Acknowledgment. This work was supported by NSF EMT grants CCF-0829797, CCF-0829798, and CCF-0523555.

Supporting Information Available: Experimental details, figure showing detailed sequence design for the fluorescence experiment, and table of DNA sequences for the demonstration of polymerase-based nanotransportation device. This material is available free of charge via the Internet at http://pubs.acs.org.

References

(1) http://www.neb.com/nebecomm/products/faqproductm0269.asp.
(2) Adleman, L. Molecular computation of solutions to combinatorial problems. *Science* **1994**, *266*, 1021–1024.
(3) Alberti, P.; Mergny, J. L. DNA duplex−quadruplex exchange as the basis for a nanomolecular machine. *Proc. Natl. Acad. Sci. U.S.A.* **2003**, *100*, 1569–1573.
(4) Baner, J.; Nilsson, M.; Mendel-Hartvig, M.; Landegren, U. Signal amplification of padlock probes by rolling circle replication. *Nucleic Acids Res.* **1998**, *26*, 5073–5078.
(5) Bath, J.; Green, S. J.; Turberfield., A. J. A free-running DNA motor powered by a nicking enzyme. *Angew. Chem., Int. Ed.* **2005**, *44*, 4358–4361.
(6) Benenson, Y.; Adar, R.; Paz-Elizur, T.; Livneh, Z.; Shapiro, E. DNA molecule provides a computing machine with both data and fuel. *Proc. Natl. Acad. Sci. U.S.A.* **2003**, *100*, 2191–2196.
(7) Benenson, Y.; Gil, B.; Ben-Dor, U.; Adar, R.; Shapiro, E. An autonomous molecular computer for logical control of gene expression. *Nature* **2004**, *429*, 423–429.
(8) Benenson, Y.; Paz-Elizur, T.; Adar, R.; Keinan, E.; Livneh, Z.; Shapiro, E. Programmable and autonomous computing machine made of biomolecules. *Nature* **2001**, *414*, 430–434.
(9) Berman, A. J.; Kamtekar, S.; Goodman, J. L.; de Vega, J. M. L. M.; Blanco, L.; Salas, M.; Steitz, T. A. Structures of phi29 DNA polymerase complexed with substrate: the mechanism of translocation in b-family polymerases. *EMBO J.* **2007**, *26*, 3494–3505.
(10) Chelyapov, N.; Brun, Y.; Gopalkrishnan, M.; Reishus, D.; Shaw, B.; Adleman, L. DNA triangles and self-assembled hexagonal tilings. *J. Am. Chem. Soc.* **2004**, *126*, 13924–13925.
(11) Chen, Y.; Mao, C. Putting a brake on an autonomous DNA nanomotor. *J. Am. Chem. Soc.* **2004**, *126*, 8626–8627.
(12) Chen, Y.; Wang, M.; Mao, C. An autonomous DNA nanomotor powered by a DNA enzyme. *Angew. Chem., Int. Ed.* **2004**, *43*, 3554–3557.
(13) Feng, L.; Park, S. H.; Reif, J. H.; Yan, H. A two-state DNA lattice switched by DNA nanoactuator. *Angew. Chem., Int. Ed.* **2003**, *42*, 4342–4346.
(14) Gelles, J.; Landick, R. RNA polymerase as a molecular motor. *Cell* **1998**, *93*, 13–16.
(15) Goel, A.; Astumian, R. D.; Herschbach, D. Tuning and switching a DNA polymerase motor with mechanical tension. *Proc. Natl. Acad. Sci. U.S.A.* **2003**, *100*, 9699–9704.
(16) Kamtekar, S.; Berman, A. J.; Wang, J.; de Vega, J. M. L. M.; Blanco, L.; Salas, M.; Steitz, T. A. Insights into strand displacement and processivity from the crystal structure of the protein-primed DNA polymerase of bacteriophage phi29. *Mol. Cell* **2004**, *16*, 609–18.
(17) Kamtekar, S.; Berman, A. J.; Wang, J.; de Vega, J. M. L. M.; Blanco, L.; Salas, M.; Steitz, T. A. The phi29 DNA polymerase: protein-primer structure suggests a model for the initiation to elongation transition. *EMBO J.* **2006**,
(18) LaBean, T. H.; Yan, H.; Kopatsch, J.; Liu, F.; Winfree, E.; Reif, J. H.; Seeman, N. C. Construction, analysis, ligation and self-assembly of DNA triple crossover complexes. *J. Am. Chem. Soc.* **2000**, *122*, 1848–1860.
(19) Li, J.; Tan, W. A single DNA molecule nanomotor. *Nano Lett.* **2002**, *2*, 315–318.
(20) Liu, D.; Balasubramanian, S. A proton fuelled DNA nanomachine. *Angew. Chem., Int. Ed.* **2003**, *42*, 5734–5736.
(21) Liu, D.; Wang, M.; Deng, Z.; Walulu, R.; Mao, C. Tensegrity: Construction of rigid DNA triangles with flexible four-arm DNA junctions. *J. Am. Chem. Soc.* **2004**, *126*, 2324–2325.
(22) Liu, Q.; Wang, L.; Frutos, A. G.; Condon, A. E.; Corn, R. M.; Smith, L. M. DNA computing on surfaces. *Nature* **2000**, *403*, 175–179.
(23) Mao, C.; LaBean, T. H.; Reif, J. H.; Seeman, N. C. Logical computation using algorithmic self-assembly of DNA triple-crossover molecules. *Nature* **2000**, *407*, 493–496.
(24) Mao, C.; Sun, W.; Seeman, N. C. Designed two-dimensional DNA holliday junction arrays visualized by atomic force microscopy. *J. Am. Chem. Soc.* **1999**, *121*, 5437–5443.
(25) Mao, C.; Sun, W.; Shen, Z.; Seeman, N. C. A DNA nanomechanical device based on the B-Z transition. *Nature* **1999**, *397*, 144–146.
(26) Niemeyer, C. M.; Adler, M. Nanomechanical devices based on DNA. *Angew. Chem., Int. Ed.* **2002**, *41*, 3779–3783.
(27) Nilsson, M.; Malmgren, H.; Samiotaki, M.; Kwiatkowski, M.; Chowdhary, B. P.; Landegren, U. Padlock probes: circularizing oligonucleotides for localized DNA detection. *Science* **1994**, *265*, 2085–2088.
(28) Park, S. H.; Pistol, C.; Ahn, S. J.; Reif, J. H.; Lebeck, A. R.; Dwyer, C.; LaBean, T. H. Finite-size, fully addressable DNA tile lattices formed by hierarchical assembly procedures. *Angew. Chem., Int. Ed.* **2006**, *45*, 735–739.
(29) Reif, J. H. The design of autonomous DNA nanomechanical devices: Walking and rolling DNA. *The 8th International Meeting on DNA Based Computers (DNA 8)*, 2002.
(30) Reif, J. H. The design of autonomous DNA nanomechanical devices: Walking and rolling DNA. *Lect. Notes Comput. Sci.* **2003**, *2568*, 22–37. Published in: Reif, J. H. *Natural Computing* **2003**, *2*, 439–461.
(31) Reif, J. H.; Sahu, S. *Autonomous programmable DNA nanorobotic devices using DNAzymes*; Technical Report CS-2007-06, Duke University, Computer Science Department, **2007**.
(32) Rodr, I.; Berman, A. J.; Wang, J.; Steitz, T. A.; Salas, M.; de Vega, M. A specific subdomain in phi29 dna polymerase confers both processivity and strand-displacement capacity. *Proc. Natl. Acad. Sci. U.S.A.* , *102*, 6407–12.
(33) Rothemund, P. W. K. Folding DNA to create nanoscale shapes and patterns. *Nature* **2006**, *440*, 297–302.
(34) Seeman, N. C. De novo design of sequences for nucleic acid structural engineering. *J. Biomol. Struct. Dyn.* **1990**, *8*, 573–581.
(35) Sha, R.; Liu, R.; Millar, D. P.; Seeman, N. C. Atomic force microscopy of parallel DNA branched junction arrays. *Chem. Biol.* **2000**, *7*, 743–751.
(36) Sherman, W. B.; Seeman, N. C. A precisely controlled DNA biped walking device. *Nano Lett.* **2004**, *4*, 1203–1207.
(37) Shin, J. S.; Pierce, N. A. A synthetic DNA walker for molecular transport. *J. Am. Chem. Soc.* **2004**, *126*, 10834–10835.
(38) Simmel, F. C.; Yurke, B. Using DNA to construct and power a nanoactuator. *Phys. Rev. E* **2001**, *63*, 041913.
(39) Simmel, F. C.; Yurke, B. A DNA-based molecular device switchable between three distinct mechanical states. *Appl. Phys. Lett.* **2002**, *80*, 883–885.
(40) Spirin, A. S. Rna polymerase as a molecular machine. *Mol. Biol.* **2002**, *36*, 153–159.
(41) Thomen, P.; Lopez, P. J.; Heslot, F. Unravelling the mechanism of rna-polymerase forward motion by using mechanical force. *Phys. Rev. Lett.* **2005**, 94.

(42) Tian, Y.; He, Y.; Chen, Y.; Yin, P.; Mao, C. A DNAzyme that walks processively and autonomously along a one-dimensional track. *Angew. Chem., Int. Ed.* **2005**, *44*, 4355–4358.
(43) Tian, Y.; Mao, C. Molecular gears: A pair of DNA circles continously rolls against each other. *J. Am. Chem. Soc.* **2004**, *126*, 11410–11411.
(44) Turberfield, A. J.; Mitchell, J. C.; Yurke, B.; Mills, J. A. P.; Blakey, M. I.; Simmel, F. C. DNA fuel for free-running nanomachines. *Phys. Rev. Lett.* **2003**, *90*, 118102.
(45) Turberfield, A. J.; Yurke,B.; Mills, J. A. P. DNA hybridization catalysts and molecular tweezers. *DNA5*, **2000**
(46) Wang, M. D.; Schnitzer, M. J.; Yin, H.; Landick, R.; Gelles, J.; Block, S. M. Force and velocity measured for single molecules of RNA polymerase. *Science* **1998**,
(47) Winfree, E. Complexity of restricted and unrestricted models of molecular computation. In *DNA Based Computers 1*; Lipton, R. J., Baum, E., Eds.; American Mathematical Society: Providence, RI, 1996; Vol. 27 of DIMACS, pp 187−198.
(48) Winfree, E. *Simulation of computing by self-assembly*. Technical Report 1998.22, Caltech, **1998**.
(49) Winfree, E.; Liu, F.; Wenzler, L. A.; Seeman, N. C. Design and self-assembly of two-dimensional DNA crystals. *Nature* **1998**, *394* (6693), 539–544.
(50) Winfree, E.; Yang, X.; Seeman, N. C. Universal computation via self-assembly of DNA: Some theory and experiments. In *DNA Based Computers II*; Landweber, L., Baum, E., Eds.; American Mathematical Society: Providence, RI, 1999; Vol. 44 of DIMACS, pp 191−213.
(51) Yan, H.; LaBean, T. H.; Feng, L.; Reif, J. H. Directed nucleation assembly of DNA tile complexes for barcode-patterned lattices. *Proc. Natl. Acad. Sci. U.S.A.* **2003**, *100* (14), 8103–8108.
(52) Yan, H.; Park, S. H.; Finkelstein, G.; Reif, J. H.; LaBean, T. H. DNA-templated self-assembly of protein arrays and highly conductive nanowires. *Science* **2003**, *301* (5641), 1882–1884.
(53) Yan, H.; Zhang, X.; Shen, Z.; Seeman, N. C. A robust DNA mechanical device controlled by hybridization topology. *Nature* **2002**, *415*, 62–65.
(54) Yin, P.; Turberfield, A. J.; Reif, J. H. *Designs of autonomous unidirectional walking DNA devices*. Technical Report CS-2004-01, Duke University, Computer Science Department, **2004**.
(55) Yin, P.; Yan, H.; Daniell, X. G.; Turberfield, A. J.; Reif, J. H. A unidirectional DNA walker moving autonomously along a linear track. *Angew. Chem., Int. Ed.* **2004**, *43*, 4906–4911.
(56) Yurke, B.; Mills, A.; Turberfield, A. A molecular machine made of and powdered by DNA. *Biophysics* **2000**, *78*, 2629.
(57) Yurke, B.; Turberfield, A.; Mills, J. A.P.; Simmel, F.; Neumann, J. A DNA-fueled molecular machine made of DNA. *Nature* **2000**, *406*, 605–608.

NL802294D